Practical results of ADRC applied to Radial Position Control of a Bearingless Induction Machine

Rodrigo TEIXEIRA [a], Werbet SILVA [b], Jossana FERREIRA [a], José PAIVA [c], Andrés SALAZAR [a], Andre L MAITELLI [a]

a Universidade Federal do Rio Grande do Norte, Natal-RN, Brazil,

rodrigoandradeteixeira@gmail.com, jossana.ferreira@ufrn.br, andres@dca.ufrn.br, maitelli@dca.ufrn.br

b Instituto Federal de Brasília, Taguatinga-DF, Brazil, werbethluizz@hotmail.com

c Instituto Federal do Rio Grande do Norte, Natal-RN, Brazil, jalvaro.paiva@gmail.com

Abstract

A Bearingless Induction Machine (BIM) with split winding has an operation strongly dependent on well-designed control routines, since the magnetic shaft suspension is a naturally unstable system. Furthermore, this system is multivariable, non-linear, and it has coupling between variables. Because of this, linear position usually presents some limitations in dealing with the system complexity. In recent years the Active Disturbance Rejection Control (ADRC) has been used to control several types of systems and has shown good results in the control of systems with strong uncertainties and nonlinearities. The main idea of the ADRC is to group all the uncertainties of the plant, such as non-modeled dynamics, external disturbances, and variations in parameters, as an additional state variable to be estimated in real-time using the input and output variables. Thus, the additional state variable can be estimated and compensated in the control loop. In the work of Silva (2021) the control of a BIM with split winding with ADRC as position controller was proposed and results from a simulated system were shown. In this work, the results obtained by Silva (2021) were improved with experimental results, using a simplified version of the ADRC controllers and a BIM with a reduced driving scheme. The results showed it is possible to use the ADRC with a split winding BIM and will be the basis for future improvements on the control strategy.

Keywords: *ADRC, position controller, bearingless induction machine, split winding.*

1. Introduction

In the last two decades, magnetic bearing technology has attracted significant attention from professionals and researchers due to its potential to perform in high-speed applications in environments where maintenance routines are more complicated. Magnetic bearing technology has been applied in different types of electrical machines. The induction motor is often chosen due to its robustness, simplicity, and low cost.

In [2], an induction motor with magnetic bearings was proposed, where the group of coils that generates rotational torque also generates radial forces. This structure is known as split winding and simplifies operation in addition to improves the utilization of the motor's internal space. The same approach was used in [3] for a three-phase induction motor, resulting in a system capable of generating higher radial forces.

The magnetic suspension of a machine shaft is a naturally unstable dynamic with multiple variables, nonlinearities, and couplings [4]. In this sense, linear controllers may not achieve a sufficiently fast and stable response for proper suspension. The use of microprocessors and power electronic devices allows the application of advanced control theories such as predictive control, sliding mode control, neural network control, fuzzy control, and others [5]. In recent years, ADRC has proven to be a promising control alternative due to its simplicity and ability to handle model uncertainties, nonlinearities, and disturbances [6]. ADRC groups unmodeled dynamics, parameter variations, and external disturbances into a variable estimated in real-time by an extended state observer (ESO) and utilizes this estimation to compensate for their effects on the control loop.

In [1], the first phase of the project was carried out which aimed to apply the ADRC technique to the radial position control of an induction machine with split winding and magnetic suspension. On this occasion, the application of the linear and nonlinear ADRC structures in the shaft position control was simulated. This paper shows the practical results of applying an extended nonlinear state observer to a split-winding induction machine.

2. Bearingless Machine with Split Winding

In the stator of the prototype used, there are three groups of windings divided to generate radial force and torque. The coils are distributed in the stator as shown illustratively in Figure 1 (a). As an example, phase A is divided into A1 and A2. When the same current (I_a) flows through coils A1 and A2, a magnetic flux is created, as represented in Figure 1 (b) by solid blue lines. When the current increases by Δi_a in coil A1 and simultaneously decreases by Δi_a in coil A2, the flux density increases on one side of the rotor while it decreases on the opposite direction with the same magnitude. The unbalance in the original flux generated by Δia generates radial force in the positive direction of the axis X. Likewise, it occurs in the opposite direction when the additional current is added to coil A2 and subtracted from coil A1.

Extending this mode of operation to the three phases and decomposing the coordinate system of the position of the coils as shown in Figure 1 in the coordinate system xy, it is possible to control the radial position in the entire bounded plane for xy.

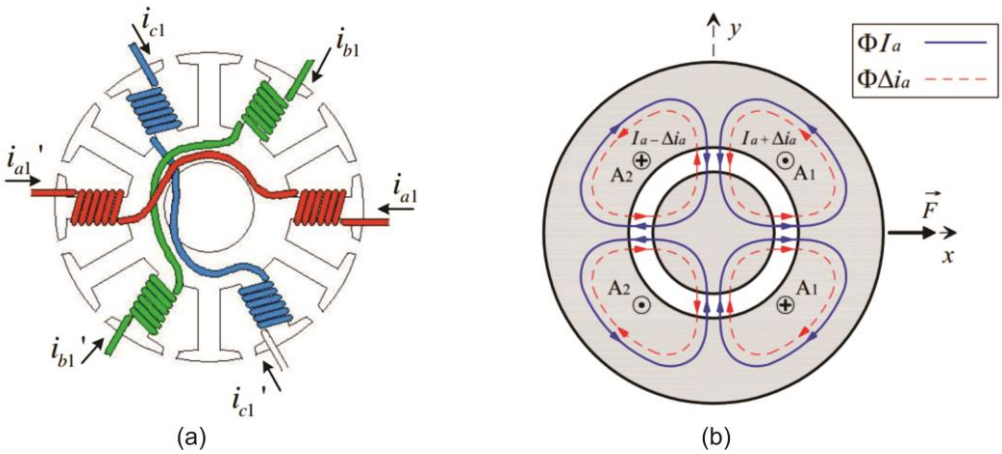

Figure 1 (a) windings distribution (b) radial forces generation.

The prototype used works vertically and is supported on the lower end of the shaft by a pivoted bearing that prevents radial and axial movements but allows angular movements. This type of system has two degrees of freedom for position control and the rotor displacement occurs in the directions of the x and y-axes.

From the application of the second law of motion to Figure 2, [7] developed a linear dynamic representation for the rotor radial displacement system. In this dynamic representation represented in Equation 1, $y(t)$ represents the radial displacement in each of the axes, $u(t)$ represents the input current signal conditioned by the control action, and $w'(t)$ is an output disturbance.

$$\ddot{y}(t) = 8374y(t) + 3680000u(t) + w'(t) \quad (1)$$

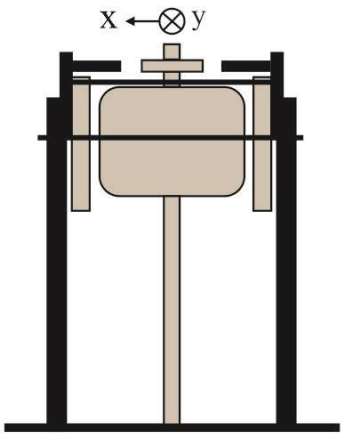

Figure 2 Machine diagram.

3. ADRC

The first version of the Active Disturbance Rejection Control (ADRC) was presented in full in Chinese by its inventor, Jingqing Han, in a work entitled “Auto disturbances rejection controller and its applications” in 1998 [8]. According to [9], “ADRC is a robust control strategy in which unknown dynamics and external disturbances are estimated and discarded in real-time, forcing the real system to behave as an approximate model. The idea is to combine internal and external disturbances as a variant parameter in the single time, the total disturbance, and use it as a fictitious state variable”.

3.1 ADRC Concept

Although ADRC is applicable to systems of order n, linear and nonlinear systems, variant and time-invariant systems, and systems with multiple inputs and outputs, for the sake of simplicity its basic concepts have been shown using the second-order dynamics represented in Equation 2. In this equation, $y(t)$ represents the output position of a controlled object, b is a constant, $u(t)$ is the input force, $w(t)$ represents external disturbances, and $f(y(t), \dot{y}(t), w(t), t)$ represents the combined effects of internal dynamics and external disturbances on the object's acceleration.

$$\ddot{y}(t) = f(y(t), \dot{y}(t), w(t), t) + bu(t) \tag{2}$$

Adopting a disturbance rejection mechanism, the process represented in Equation 2 can be viewed as a double integrator plant, with gain b, and disturbed by $f(y(t), \dot{y}(t), w(t), t)$. The term $f(y(t), \dot{y}(t), w(t), t)$ is defined as generalized disturbance and in ADRC is the focus of the control design.

By specifying $\hat{f}$ as an estimate of the generalized disturbance at time instant t, the input represented in Equation 3 reduces expression 2 to the easily controllable double integrator of expression 4.

$$u(t) = (-\hat{f} + u_0)/b \tag{3}$$

$$\ddot{y}(t) = u(t) \tag{4}$$

The main difference between this approach and model-based approaches is that ADRC assumes no analytical expression for $f(y(t), \dot{y}(t), w(t), t)$.

3.2 Extended State Observer

The extended state observer proposed by J. Han [10] became practical through the tuning method proposed in [11] which simplified its implementation. The idea is based on using an extended state space model of Equation 2 that includes the generalized disturbance $f(y(t), \dot{y}(t), w(t), t)$ as an additional state. Considering the system output $y(t)$ as state $x_1(t)$, the output derivative $\dot{y}(t)$ as state $x_2(t)$, and the derivative of $\dot{y}(t)$ as extended state $x_3(t)$, this state becomes approximately equal to the generalized disturbance $f(y(t), \dot{y}(t), w(t), t)$.

Thus, a state observer with appropriately selected gains provides an estimation of the states $x_1(t)$, $x_2(t)$, and $x_3(t)$. Consequently, it provides an estimation of the generalized disturbance through the extended state $x_3(t)$. With the estimation of $f(y(t), \dot{y}(t), w(t), t)$ from the extended state $x_3(t)$ it is possible to use the input shown in Equation 3 and reduce the system to the double integrator of Equation 4.

The original structure of an ADRC controller is composed of a Tracking Differentiator (TD) block, an Extended State Observer (ESO), and a non-linear control structure block. In this work, the TD structure was not used.

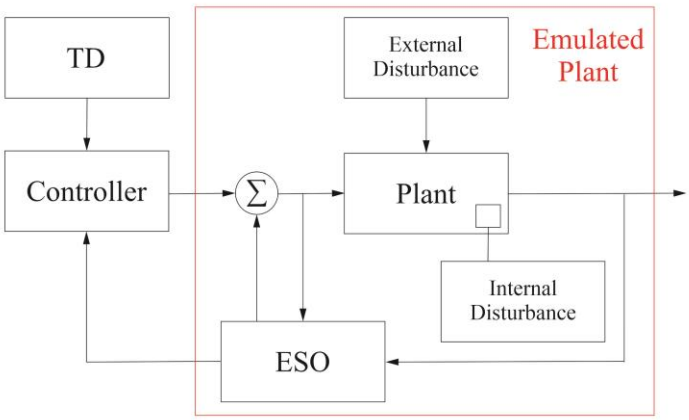

Figure 3 ADRC general diagram.

3.3 NLESO Structure

In the ESO structure, the generalized disturbance $f(y(t), \dot{y}(t), w(t), t)$ is considered an additional state of the system.

$$\begin{aligned} \dot{x}_1(t) &= x_2(t) \\ \dot{x}_2(t) &= x_3(t) + b_0 u(t) \\ \dot{x}_3(t) &= h \\ y(t) &= x_1(t) \end{aligned} \tag{5}$$

Where $x_3(t) = f(y(t), \dot{y}(t), w(t), t)$ is the augmented state and $h = \hat{f}$, its derivative. h is seen as an unknown disturbance. The above system can be rewritten in state space by:

$$\begin{aligned} \dot{x}(t) &= \boldsymbol{A}x(t) + \boldsymbol{B}u(t) + \boldsymbol{E}h(t) \\ y(t) &= \boldsymbol{C}z(t) \end{aligned} \tag{6}$$

Where:

$$\boldsymbol{A} = \begin{bmatrix} 0 & 1 & 0 \\ 0 & 0 & 1 \\ 0 & 0 & 0 \end{bmatrix}, \qquad \boldsymbol{B} = \begin{bmatrix} 0 \\ b_0 \\ 0 \end{bmatrix}, \qquad \boldsymbol{C} = [1 \quad 0 \quad 0], \qquad \boldsymbol{E} = \begin{bmatrix} 0 \\ 0 \\ 1 \end{bmatrix}.$$

From the extended representation of the system, an observer can be constructed to estimate numerical values for $z_1(t)$, $z_2(t)$ and $z_3(t)$, which are respectively the estimated values of the states $x_1(t)$, $x_2(t)$ and $x_3(t)$. The work [12] proposed a nonlinear structure for the ESO. This structure is referred to as NLESO and can be written mathematically as:

$$\begin{aligned} \dot{z}_1(t) &= z_2(t) - \beta_1 fal(e, \alpha_1, d_1) \\ \dot{z}_2(t) &= z_3(t) - \beta_2 fal(e, \alpha_2, d_2) + b_0 u(t) \\ \dot{z}_3(t) &= -\beta_3 fal(e, \alpha_3, d_3) \end{aligned} \tag{7}$$

Where β_1, β_2 and β_3 are the observer gains and $fal(e, \alpha, d)$ is a nonlinear function, defined by:

$$fal(e, \alpha, d) = \begin{cases} |e|^{\alpha} sgn(e), & |e| > d \\ e/d^{1-\alpha}, & |e| > d \end{cases} \tag{8}$$

the value of e is the error between the system output and its estimate and α and d are turning parameters. The block diagram of the NLESO applied to a generic second-order plant is shown in Figure 4.

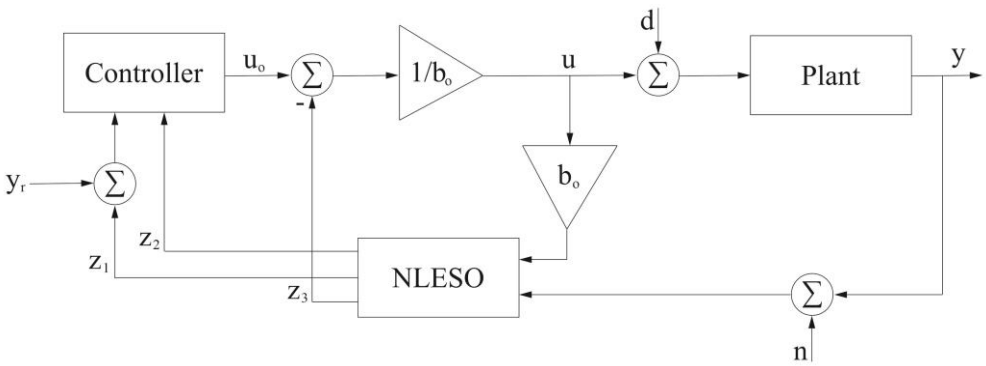

Figure 4 Block Diagram of an ADRC control loop.

4. Description of the System

Figure 5 provides an overview of the experimental bench used in the work. The equipment was grouped into the following blocks: monitoring and control, power supply, and bearingless machine. The bearingless machine block consists of the bearingless electric induction machine on which the tests were performed. The power supply circuit block comprises the entire infrastructure of electronic components and equipment responsible for providing the power supply at the appropriate levels to control the machine variables. The monitoring and control block consists of the electronic circuits, processors, algorithms, and monitoring devices that were necessary to implement the system's control and supervision routines. The variable i_{abxy} represents the four-phase electrical connections that allow the drive block to supply controlled electrical currents to the bearing motor. Figure 5 also indicates the reading of these i_{abxy} currents

performed by the monitoring and control block. The variable Δxy represents the signals corresponding to the radial positions of the x and yy axes of the bearing motor using by the monitoring and control block. Finally, the arrow named *PWM* indicates the signals sent by the monitoring and control block to the drive block.

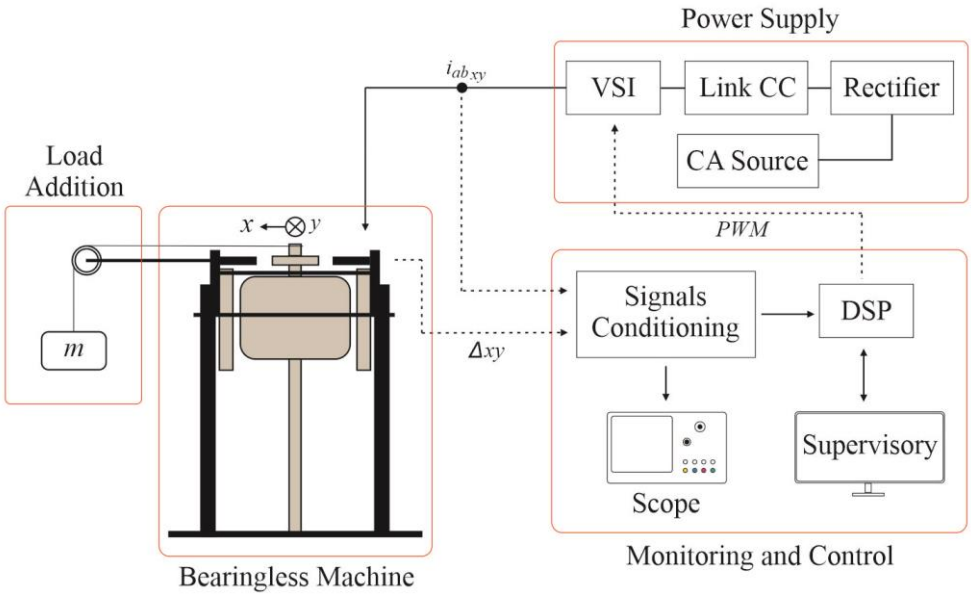

Figure 5 Components of the experimental bench.

Figure 6 shows a real image of the experimental bench. This structure is in the Laboratory in the Computer and Automation Engineering Department at UFRN.

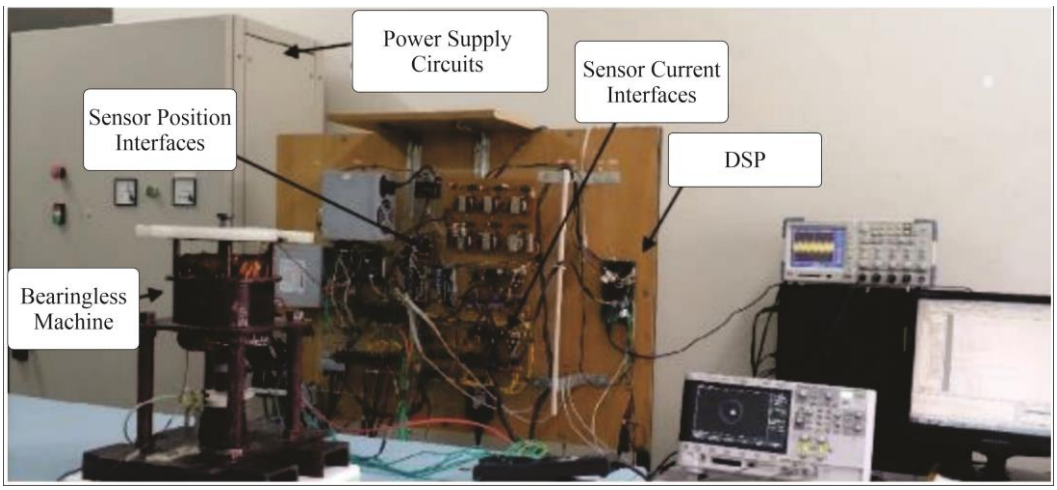

Figure 6 Experimental bench.

5. Results

From the simulated results by Silva (2021) it could be seen that ADRC with the linear and nonlinear structure are successful in providing a stable response to the system. However, the nonlinear structure of the ADRC exhibits a faster and more damped response in the presence of disturbances. For this reason, this structure was used in obtaining the practical results shown in this paper.

Figure 7 shows the response of the radial position control in the x and y directions with ADRC controllers in two different moments. At first, the y direction is set constant and the x position is variable (Figures 7(a) and 7(b)), then, the x direction is set constant and y position is variable (Figures 7(c) and 7(d)). The results obtained during this test show that step variations in one of the controlled axes do not have a significant influence on the dynamic behavior of the opposite axis.

To analyze the robustness of the controller to external disturbances an apparatus as shown in Figure 5 was used. The states z_1, z_2 and z_3 of the x and y axes were obtained at a time interval that allowed the instant of adding radial

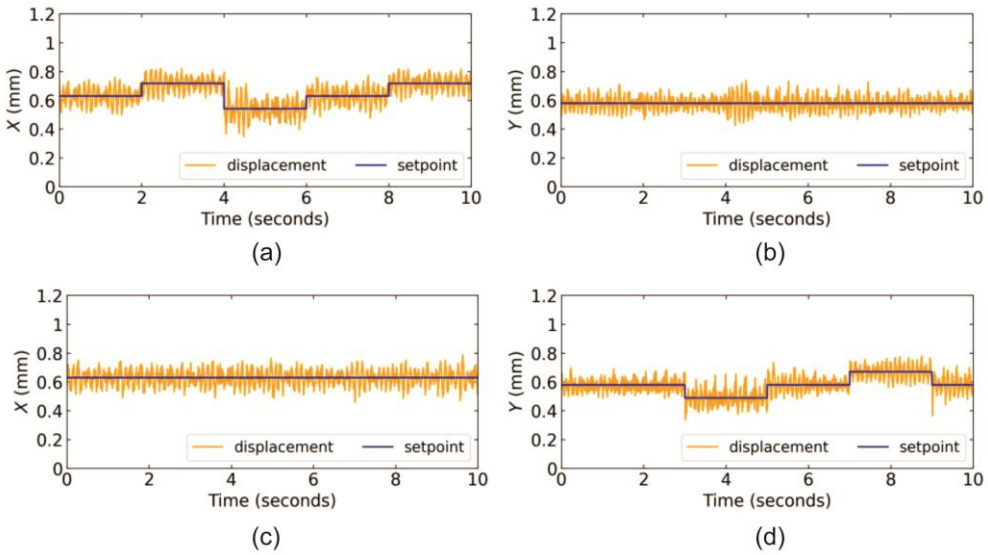

Figure 7 Rotor radial position with ADRC.
(a) X position with a constant reference (b) Y position with a constant reference.
(b) X position with a constant reference (d) Y position with a variable reference.

load to the machine shaft to be detected. In each graph in Figure 8, a dashed vertical line was inserted to indicate the instant of application of 150 grams aligned with the x-axis.

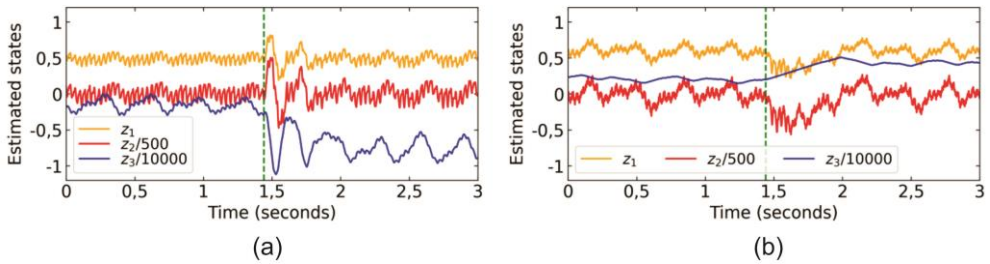

Figure 8 Estimated states behavior for NLESO under radial load application.
(a) X-axis states. (b) Y-axis states.

Considering the states z_1- x and y position, z_2 - derivative of z_1, and z_3 - derivative of z_2, it is possible to conclude by observing the z_1 states in Figures 8 (a) and (b) the controller was little influenced by the application of radial load, since the response was similar before and after the addition of the disturbance. The behavior of the states also indicated an aggressive reaction of the controller in the transient regime, which resulted in high z_2 values during this region in the graphs. Finally, the change in the mean value of z_3 indicates that the extended observer was able to identify the addition of the external disturbance inserted into the system.

6. Conclusions

In this paper, the application of the ADRC active disturbance rejection technique to a bearingless induction machine was analyzed. The results discussed were obtained using a nonlinear framework for the extended state estimator. The results for reference variation show good dynamic decoupling between the x and y axes. The test with load imposition showed that the implemented nonlinear observer was able to detect the generalized disturbance and maintained the average value at the output before and after load application. Finally, the results obtained show the success of the ADRC technique in the active estimation and rejection of disturbances in the radial positioning process of a split rotor bearingless machine.

7. Acknowledgments

This work was supported by Comissão de Aperfeiçoamento de Pessoal do Nível Superior (CAPES) and Programa de Pós-graduação em Engenharia Elétrica e de Computacão (PPgEEC/UFRN).

References

[1] Silva, Werbet, et al. “Application of Active Disturbance Rejection Control (ADRC) in the Radial Position Control of a Bearingless Induction Machine With Split Winding” Proc. 17th ISMB. 2021.

[2] A.O. Salazar and R.M. Stephan. A bearingless method for induction machines. IEEE Transactions on Magnetics, 29(6):2965–2967, 1993.

[3] Jossana Maria de Souza Ferreira. Modelagem de máquina de indução trifásica sem mancais com bobinado dividido. 2006.

[4] Zebin Yang, Chengling Lu, Xiaodong Sun, Jialei Ji, and Qifeng Ding. Study on active disturbance rejection control of a bearingless induction motor based on an improved particle swarm optimization–genetic algorithm. IEEE Transactions on Transportation Electrification, 7(2):694

[5] Zebin Yang, Jialei Ji, Xiaodong Sun, Huimin Zhu, and Qian Zhao. Active disturbance rejection control for bearingless induction motor based on hyperbolic tangent tracking differentiator. IEEE Journal of Emerging and Selected Topics in Power Electronics, 2019.

[6] Li Sun, Wenchao Xue, Donghai Li, Hongxia Zhu, and Zhi-gang Su. Quantitative tuning of active disturbance rejection controller for fopdt model with application to power plant control. IEEE Transactions on Industrial Electronics, pages 1–1, 2021.

[7] Francisco Elvis Carvalho Souza. Otimização da estrutura de acionamento para o controle de posição radial de um motor de indução trifásico sem mancais com enrolamento dividido. 2018.

[8] Huang, Deqing, Da Min, Yupei Jian & Yanan Li (2019), ‘Current-cycle iterative learning control for high-precision position tracking of piezoelectric actuator system via active disturbance rejection control for hysteresis compensation’, IEEE Trans. on Industrial Electronics.

[9] Ahmad, Saif, and Ahmad Ali. "Active disturbance rejection control of DC–DC boost converter: A review with modifications for improved performance." IET Power Electronics 12.8 (2019): 2095-2107.

[10] Han, Jingqing. "From PID to active disturbance rejection control." *IEEE transactions on Industrial Electronics* 56.3 (2009): 900-906.

[11] Gao, Zhiqiang. "Scaling and bandwidth-parameterization based controller tuning." *ACC*. 2003.

[12] Zhiqiang Gao. From linear to nonlinear control means: A practical progression. ISA transactions, 41(2):177–189, 2002.